MiR-130a-5p contributed to the progression of endothelial cell injury by regulating FAS

Wei Wang,[1,2] Wenbo Tang,[3] Erbo Shan,[4] Lei Zhang,[2] Shiyuan Chen,[3] Chaowen Yu,[3] Yong Gao[1]

[1]The First Clinical College of Jinan University, Guangzhou
[2]Surgical Oncology Department, the Second Affiliated Hospital of Bengbu Medical College, Bengbu
[3]Vascular Surgery Department, the First Affiliated Hospital of Bengbu Medical College, Bengbu
[4]General Surgery Department, the Second Affiliated Hospital of Bengbu Medical College, Bengbu, China

ABSTRACT

MicroRNAs (miRNAs) play critical roles in the development of vascular diseases. However, the effects of miR-130a-5p and its functional targets on atherosclerosis (AS) are still largely unknown. In this regard, our aim is to explore the potentially important role of miR-130a-5p and its target gene during the progression of endothelial cell injury. We first found oxidized low-density lipoprotein (ox-LDL) induced FAS and cell apoptosis in HUVECs. Subsequently, miR-130a-5p expression was verified to be downregulated after ox-LDL treatment and negatively correlated with FAS, and FAS was identified as substantially upregulated in the ox-LDL-treated HUVEC cells. After that, the knockdown of FAS and overexpression of miR-130a-5p together were observed to aggregate ox-LDL-induced reduction of cell viability and apoptosis, cell cycle progression, cell proliferation, cell migration and invasion. In conclusion, we detected that miR-130a-5p contributed to the progression of endothelial cell injury by regulating of FAS, which may provide a new and promising therapeutic target for AS.

Key words: Atherosclerosis; ox-LDL; miR-130a-5p; FAS.

Introduction

Atherosclerosis (AS), a chronic inflammatory disease, is a major cardiovascular disease that is characterized by the deposition of oxidized low-density lipoprotein (ox-LDL), endothelial cell injury, and plaque accumulation in the vascular walls.[1-4] Its prevention and treatment are all important in medical research. ox-LDL within plaques has been reported to be able to induce apoptosis of endothelial cells, and it is considered to contribute to the inflammatory state of AS and to play a key role in its pathogenesis.[5-7] It leads to considerable morbidity and mortality in most countries. However, there is still a lack of therapeutics that can effectively inhibit these abnormal features during the progression of AS. Therefore, improved understanding of the potential biological mechanisms underlying endothelial cell injury could facilitate the development of novel treatments for AS.

miRNAs, also widely found in humans, are a group of 19-22 nucleotides. They comprise of non-coding, single-stranded RNA molecules that participate in sequence-specific post-transcriptional regulation of gene expression.[8] miRNAs have emerged as crucial players in many biological processes of human diseases, such as apoptosis, cell proliferation, cell migration and invasion.[9] It has been verified that many miRNAs also play important roles in AS. For instance, miR-146-5p has been reported to protect against AS by inhibiting vascular smooth muscle cell proliferation and migration.[10] miR-200b-3p has been validated to promote endothelial cell apoptosis by targeting HDAC4 in AS.[11] miR-130a has also been confirmed to promote inflammation to accelerate AS *via* the regulation of proliferator-activated receptor γ (PPARγ) expression.[12] In addition, miR-130a-5p has been observed to an play important role during the early stages of obesity development.[13] However, it is still unclear about the potentially important role of miR-130a-5p during the development of AS.

FAS (also known as APO-1 or CD95) belongs to the subgroup of the tumor necrosis factor receptor (TNF-R) family that contain an intracellular 'death domain' and can trigger apoptosis cell surface death receptor.[14] Activated FAS recruits FAS-associated protein death domain (FADD) adaptor protein. FADD further recruits caspase-8, caspase-10, and cellular FADD-like interleukin-1-β-converting enzyme-inhibitory protein (c-FLIP) to form the death-inducing signaling complex (DISC), which mediates both apoptotic and non-apoptotic signaling pathways.[15,16] However, to date, little is known about the important role of miR-130a-5p and FAS, and this needs to be further explored.

In this study, we aimed to investigate the effects of miR-130a-5p and FAS on endothelial cell injury, as well as the potential molecular mechanisms involved in cultured human umbilical vein endothelial cells (HUVEC) *in vitro*.

Materials and Methods

Cell culture

HUVEC cells have played a major role as a model system for the study of the regulation of endothelial cell function. HUVEC cells (Shanghai AllCells Biotech Co., Ltd. Shanghai, China) were cultured at 37°C and 5% CO_2 in HyClone M-199 media (GE Healthcare Life Sciences, South Logan, UT, USA) with 1% antibiotics-antimicrobial (Gibco, Carlsbad, CA, USA), 15.3 units of heparin (Sigma-Aldrich, St. Louis, MO, USA), one vial of endothelial cell growth supplement (Millipore, Bedford, MA, USA), and 10% FBS (Sigma-Aldrich). Cells were cultured up to 80% confluency, and growth media was replaced every other day.

The cellular model of AS was constructed using HUVEC stimulated by 100 µg/mL of oxidized low-density lipoprotein (ox-LDL, Solarbio, Beijing, China) ox-LDL (Solarbio, Beijing, China) for 24 h.[17] Ox-LDL at 100 µg/mL was diluted in PBS.

RNA interference

For the RNA interference assay, the siFAS and negative siCtrl were from GenePharma Co., Ltd. (Shanghai, China). We tested 3 siFAS sequences. The siFAS-1 sequence was composed of the sense strand 5'-CCCUUGCACCAAAUGUGAATT-3' and the antisense strand 5'-UUCACAUUUGGUGCAAGGGTT-3'. The siFAS-2 sequence was composed of the sense strand 5'-GCCAAUUCCACUAAUUGUUTT-3' and the antisense strand 5'-AACAAUUAGUGGAAUUGGCTT-3'. The siFAS-3 sequence was composed of the sense strand 5'-GGUUCUCAUGAAUCUC-CAATT-3' and the antisense strand 5'-UUGGAGAUUCAUGA-GAACCTT-3'. The sequence of siCtrl consisted of the sense strand UUCUCCGAACGUGUCACGUTT and the antisense strand ACGUGACACGUUCGGAGAATT. HUVECs were transfected with 3 siRNAs mixture using RNAiMAX (Invitrogen, Carlsbad, CA, USA) according to the manufacturer's instructions. We seeded the cells into 6-well plate to be 80% confluent at transfection; 9 µL of RNAiMAX was diluted with 150 µL of Opti-MEM medium (Gibco); 3 µL of siRNA (10 µM) was diluted in 150 µL of Opti-MEM medium. The diluted siRNA was added to diluted RNAiMAX at 1:1 ratio and incubated for 5 min at room temperature. After that, 250 µL of siRNA-lipid complex was added into per well and incubated for 2 days at 37°C.

miR-130a-5p overexpression

Negative control oligonucleotide (miR NC) and miR-130a-5p mimic (miR mimic) overexpression lentiviral systems were commercially available at RiboBio Co. Ltd. (Guangzhou, China). Cells were plated at 30-50% confluence for 24 h. After that, 50 pmol/mL RNA oligonucleotides were transfected using the Lipofectamine 2000 reagent (Invitrogen) according to the manufacturer's instructions.

qRT-PCR

Total RNA from the cells was prepared by TRIzol reagent (Invitrogen). Then, 1 µg of total RNA was subjected to reverse transcription using PrimeScript RT Master Mix (Perfect Real Time) (Takara, Shiga, Japan). Quantitative real-time PCR was carried out using the TB Green Premix Ex Taq II (Tli RNaseH Plus) (Takara) to detect FAS gene mRNA level (forward: 5'-AGATTGTGTGATGAAGGACATGG-3', reverse: 5'-TGTTGCTGGTGAGTGTGCATT-3') on StepOnePlus Real-Time PCR System (Applied Biosystems, Waltham, MA, USA). GAPDH (forward: 5'-AGAAGGCTGGGGGCTCATTTG-3', reverse: 5'-AGGGGCCATCCACAGTCTTC-3') was used as the internal reference gene.

For miRNA quantification, the Taqman advanced miRNA cDNA synthesis kit was used to implement reverse transcription following the manufacturer's instruction (Applied Biosystems, Carlsbad, CA, USA). The Taqman microRNA reverse transcription kit was used for U6 small nuclear RNA (snRNA) to perform reverse transcription according to manufacturer's protocol (Applied Biosystems). All probes were purchased from ThermoFisher Scientific (Waltham, MA, USA). The comparative $2^{-\Delta\Delta CT}$ method[18] was used to analyze the relative expression level of FAS and miR-130a-5p.

Western blotting

The total protein of the cells was extracted with T-PER tissue protein extraction reagent (Thermo Pierce, Rockford, IL, USA)

with 1% halt protease and phosphatase inhibitor (Thermo Pierce). After that, 20 mg of the extracted protein was loaded and run on odium dodecyl sulfate-polyacrylamide gels (8-12% separating gel, 5% concentrated gel) for protein electrophoresis. The protein in the gel was transferred onto a PVDF membrane (Millipore) for antibody detection. The PVDF membrane was blocked for 1 h at room temperature in 5% non-fat milk in Tris-buffered saline with 0.1% Tween- 20 detergent (TBST). The membrane was washed by TBST for 3 times for 10 min each in room temperature and followed by incubation with primary antibodies (anti-fas, 1:1000; Abcam, Cambrigde, MA, USA) overnight at 44°C. α-tubulin served as internal control (1:5000, Abcam). Subsequently, the membrane was washed with TBST 3 times for 10 min each in room temperature, and was incubated for 1h at room temperature with horseradish peroxidase (HRP) labeled goat anti-mouse IgG or goat anti-rabbit IgG secondary antibody, respectively (Thermo Pierce). Proteins were visualized by using ECL western blotting detection reagents (SuperSignal® west dura extended duration substrate; Thermo Pierce) after the membrane was washed by TBST for 3 times for 10 min each in room temperature. The relative expression of the target protein was quantitatively analyzed by ImageJ (NIH, Bethesda, MD, USA).

Cell counting kit-8 (CCK8) assay

Cells were first transfected with siCtrl or siFAS for 24 h. Afterwards, cells with siCtrl were transfected with miR NC or miR mimic, while cells with siFAS were transfected with miR NC or miR mimic for 24 h. After being detached with 0.25% pancreatin (Biomiky, China), the cells constructed into a single cell suspension. Around 2.5×10^4 cells were taken from the cell suspension, and added to complete the medium to 2.5 mL. From D1 to D5, 10 μL of CCK-8 solution (Biomiky, China) was added to each well of a 96-well and incubated for another 2 h. The absorbance (optical density) values of each well were detected using a microplate reader at 450 nm while the reference wavelength was 650 nm. The test was performed for 5 consecutive days by adding CCK-8 at the same time point every day.

Apoptosis assay

Cell apoptosis was detected by the Annexin V FITC/PI kit (Beyotime, Shanghai, China). Cells were treated with 100 μg/mL of ox-LDL for 24 h. The cells were first transfected with siCtrl or siFAS for 24h, and then transfected with miR NC or miR mimic. Subsequently, cells were digested, centrifuged at 1,300 rpm at 4°C for 5 min and transferred to a new centrifuge tube. Cells were resuspended in ice-cold PBS and centrifuged in 1,300 rpm at 4°C for 5 min. After removal of PBS, a total of 200 μL of 1X binding buffer was added to each tube and mixed evenly; 5 μL of annexin V-FITC and 10 μL of propidium iodide (PI) was added, gently mixed and incubated at for 30 min at room temperature in the dark. After that, cells were detected by using a flow cytometer (BD Bioscience, San Jose, CA, USA).

Cell cycle assay

Cells were first treated with 100 μg/mL of ox-LDL for 24 h. Subsequently, cells were transfected with siCtrl or siFAS for 24 h. After that, the cells with siCtrl or siFAS were transfected with miR NC or miR mimic for 24 h. A cell cycle detection kit (Beyotime) was used to measure cell cycle distribution. Briefly, the cells were fixed with 70% ethanol, digested with 100 μL of RNase A for 30 min, stained with 400 μL of PI, and were incubated for 30 min in dark. Cell cycle distribution was detected and analyzed with a flow cytometer (BD Bioscience, San Jose, CA, USA).

5-ethynyl-2′-deoxy-uridine assay

The 5-ethynyl-2′-deoxy-uridine (EdU) incorporation assay (Beyotime) was performed to evaluate cell proliferation. Cells were treated with 100 μg/mL of ox-LDL for 24 h and transfected with siCtrl or siFAS for 24 h. In the next step of the study, we transfected the cells with siCtrl or siFAS with miR NC or miR mimic for 24 h, separately. Subsequently, cells were digested and seeded into a 96-well plate at a density of 2×10^3 cells per well. Cells were cultured with 20 μM of EdU diluent at 37°C with 5% CO_2 for 2 h. And then 4% paraformaldehyde was used to fix cells for 15 min. After cells were washed with PBS, 1 mL of permeabilization solution was added to per well and incubated for 15 min at room temperature. Cells were incubated with endogenous peroxidase blocking solution at room temperature for 20 min, and washed with PBS 3 times. 50uL of Click reaction solution was added into each well and incubated for 30 min at room temperature in the dark. After that, cells were washed with PBS 3 times. Streptavidin-HRP working solution was added to the sample, incubated at room temperature for 30 min, and washed with PBS 3 times. After that, 0.1 mL of TMB color developing solution was added, and incubated at room temperature for 30 min. The absorbance was directly measured at 370 nm.

Wound scratch assay analysis

Cells were treated with 100 μg/mL of ox-LDL for 24 h. After that, cells were first transfected with siCtrl or siFAS for 24 h. Next, we transfected the cells with siCtrl or siFAS with miR NC or miR mimic for 24 h. Wound scratch assay was performed as previously described.[19-22] Subsequently, cells were seeded into 12-well plates at a density of 5×10^5 cells per well with medium, and they were cultured for 24 h to reach ~90% confluence. A 10 μL pipette tip was used to make a scratch line. Cells were washed with PBS 3 times to remove the scratched cells. After that, cells were cultured in a medium containing 0.5% FBS. The cells were incubated at 37°C and images were captured at 6 and 24 h using a light microscope (Olympus Corporation, Tokyo, Japan). PBS was used as a control.

Transwell assay

Cell invasion was assayed by Boyden chamber assay with a 24-well collagen-based cell invasion assay kit (Millipore); 200 μL of serum-free medium containing 5×10^5 cells for the invasion assay were added to the filter. The bottom chamber was prepared with 750 μL of complete cell culture medium in which the FBS was a chemoattractant. After being incubated for the indicated time, the non-invasive cells were cleaned by scrubbing with a cotton swab. The cells that adhered to the outside of the membrane were fixed and dyed with Cristal Violet solution. An Olympus optical microscope (Olympus Corporation) was used to observe migratory or invasive cells.

Dual-luciferase reporter assay

The wide type (WT) and mutant (MUT) binding sites of FAS were commercially available from General Biosystems (Chuzhou, Anhui, China) and were cloned into the psiCHECK-2 vector (Promega, Madison, WI, USA) downstream of a firefly luciferase reporter gene using the XhoI and EcoRI restriction sites.

Cells were seeded in a 24-well plate (2×10^4 cells/well). After being in culture for 24 h, plasmids were transfected using the X-tremeGene HP DNA transfection reagent (Roche Diagnostic, Basel, Switzerland) and 100 μL of Opti-MEM (Gibco) at a ratio of 1 μg plasmid to 2 μL X-tremeGene HP reagent. Following incubation at 37°C for 6 h, the medium was replaced with fresh culture medium containing 10% FBS. Following incubation for 24 h, the dual-luciferase reporter assay system (Beyotime, Shanghai, China)

was used to verify the transfection efficiency according to the manufacturer's protocols.

Statistical analysis

Statistical analyses were performed using GraphPad Prism and all data were presented as mean ± SD from at least 3 independent experiments. Differences between two groups were analyzed by unpaired *t*-test. ANOVA was used to compare differences in multiple groups. A p-value of less than 0.05 is statistically significant.

Results

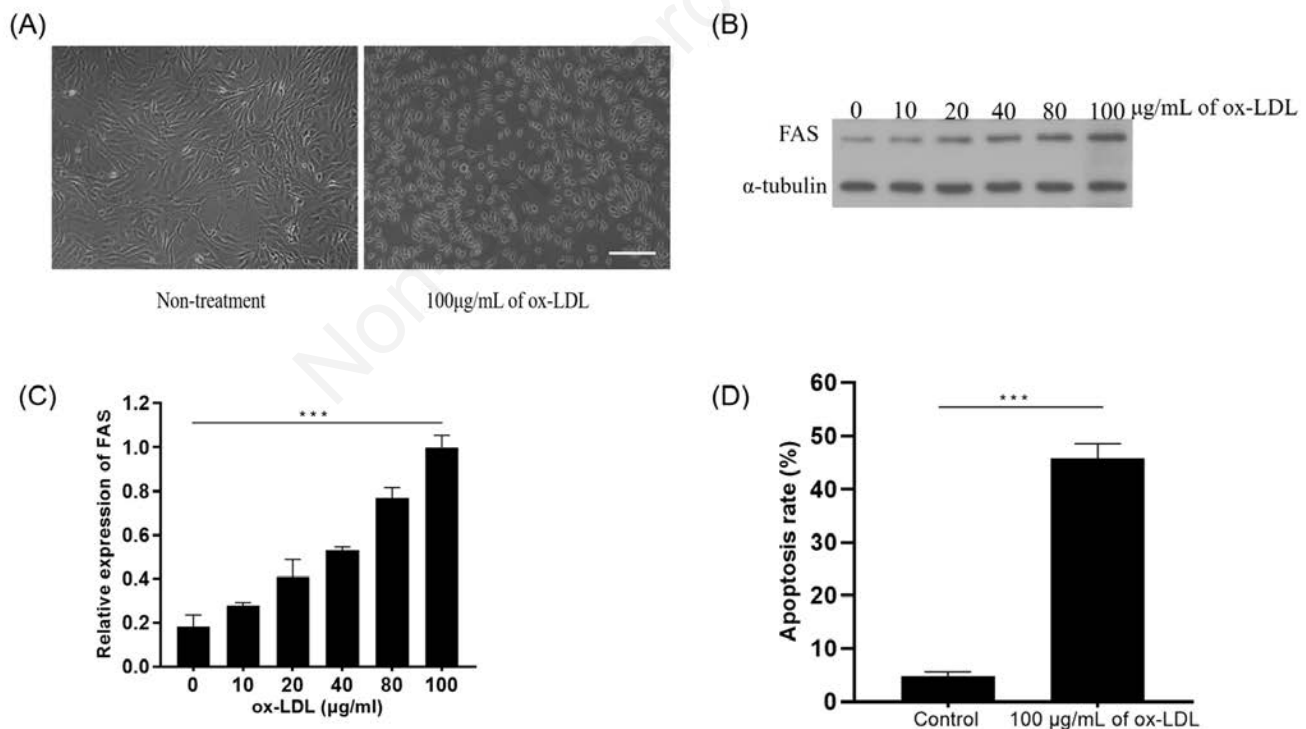### ox-LDL-induced FAS and cell apoptosis in HUVEC cells

ox-LDL was used to mimic endothelial injury caused by lipid accumulation in atherosclerosis. HUVEC cells were stimulated with several doses of ox-LDL (10, 20, 40, 80 and 100 μg/mL) for 24 h. The cell morphology changed from a spindle shape to a spherical or elliptical shape after being treated with 100 μg/mL of ox-LDL compared with the non-treatment control group (Figure 1A). Meanwhile, we found that FAS protein expression was altered by western blotting under the induction of different dose of ox-LDL (Figure 1B). As the dose of ox-LDL increased, FAS expression gradually increased (Figure 1 B,C). We also observed that HUVEC cell apoptosis was significantly increased after treatment of 100 μg/mL (Figure 1D).

FAS was repressed by miR-130a-5p

To advance the understanding of the FAS involved in ox-LDL induced HUVEC cell apoptosis and discover the potential target gene network of early AS, we first verified the upstream regulators including miRNAs for FAS. MiR-130a-5p is one of the predicted upstream miRNAs. As shown in Figure 2A, miR-130a-5p expression decreased as the dose of ox-LDL increased. FAS mRNA and miR-130a-5p expression levels are negatively correlated (Figure 2A). To verify whether FAS is a potential target of miR-130a-5p, HUVEC cells were cotransfected with the FAS 3'-UTR wide type (WT) firefly luciferase reporter vectors with miR-130a-5p (miR mimic) or control miRNA (miR NC). We also cotransfected HUVEC cells with mutant (MUT) firefly luciferase reporter vectors with miR mimic or control miR NC. We found that miR-130a-5p repressed the activity of FAS 3'-UTR WT (Figure 2B). When we mutated the binding site in FAS, inhibition of the reporter activities by miR-130a-5p was less compared with FAS 3'-UTR WT (Figure 2B). Furthermore, NC had no effect on both of FAS 3'-UTR WT and MUT (Figure 2B). These results suggest that the FAS is directly repressed by miR-130a-5p and that both are involved in the endothelial cell injury.

FAS knockdown and miR-130a-5p overexpression aggregated ox-LDL induced cell viability and apoptosis reduction

SiFAS or and miR-130a-5p mimic were transfected into HUVECs to reduce FAS expression and overexpress miR-130a-5p.

Figure 1. Ox-LDL-induced FAS and cell apoptosis in HUVECs. A) the cell morphology changed from a spindle shape to a spherical or elliptical shape after being treated with 100 g/mL of ox-LDL compared with the non-treatment control group; scale bar: 50 μm. B) Western blot analysis of FAS under different dose of Ox-LDL. C) The blotting bands were quantified by ImageJ. The relative FAS expression levels were normalized to α-tubulin; ***p<0.01 *vs* no Ox-LDL treatment. (D) 100 g/mL ox-LDL induced cell apoptosis. The apoptosis rate was detected through flow cytometry by using annexin V-FITC/PI double staining. The apoptotic rate was analyzed in terms of the percentage of the lower and upper right quadrants. Results are mean ± SD (n = 3). ***p<0.01 *vs* control.

HUVECs transfected with control siRNA and miRNA were treated with 100 μg/mL ox-LDL for 24h. These samples constituted the control group. The same control group was used in all of the subsequent assays. The effect of siFAS and miR-130a-5p mimic on the ox-LDL-induced reduction of HUVEC viability was detected with CCK-8. Figure 3A showed that the cell viability in the siFAS group or miR-130a-5p mimic with ox-LDL treatment was increased compared with the control group. The cell viability of the siFAS and miR-130a-5p mimic group with ox-LDL treatment was significantly increased more compared to either siFAS group or miR-130a-5p mimic group (Figure 3A).

The effect of siFAS and miR-130a-5p mimic on the ox-LDL-induced reduction of HUVEC apoptosis was determined by flow cytometry. We found that the cell apoptosis in the siFAS group or

miR-130a-5p mimic with ox-LDL treatment was significantly decreased compared with the control group (Figure 3B). The cell apoptosis of the siFAS and miR-130a-5p mimic group with ox-LDL treatment was strongly decreased more compared to either siFAS group or miR-130a-5p mimic group (Figure 3B).

FAS knockdown and miR-130a-5p overexpression promoted cell cycle at S and G2/M phases

We subsequently examined the effect of FAS knockdown and miR-130a-5p overexpression on cell cycle progression. In ox-LDL treatment cells, the percentage of HUVECs in the G1 phase was obviously decreased in siFAS and miR-130a-5p mimic groups compared with that in control group, whereas the percentage of siFAS and miR-130a-5p mimic group was signifi-
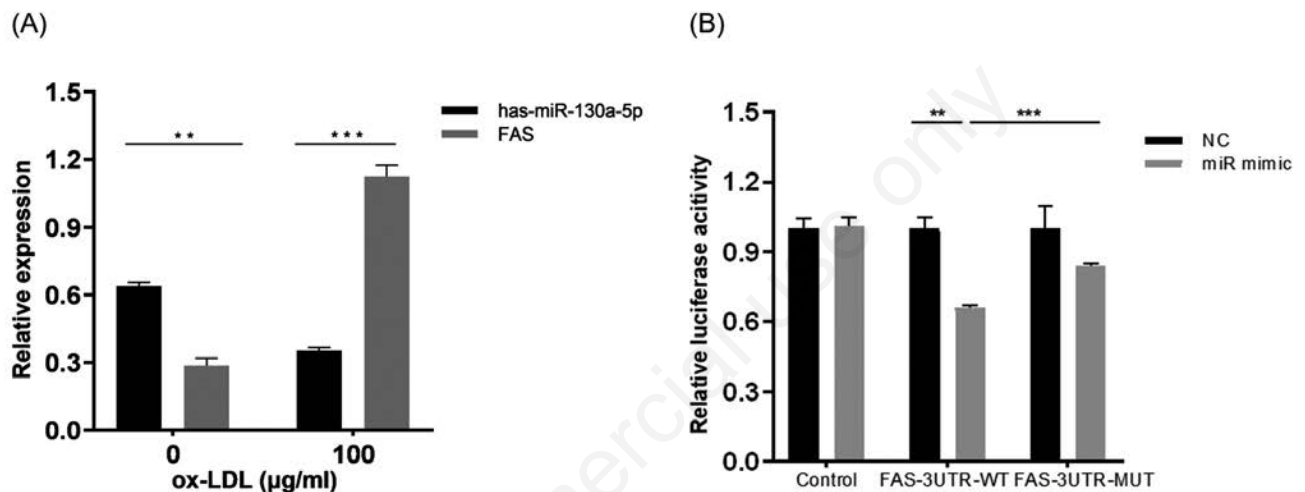
Figure 2. FAS was repressed by miR-130a-5p. A) miR-130a-5p expression decreased as the dose of ox-LDL increased. FAS mRNA and miR-130a-5p expression levels are negatively correlated; results are mean ± SD (n=3); **p<0.05 vs miR-130a-5p; ***p<0.01 *vs* miR-130a-5p. B) 3'-UTR luciferase reporter assays. HUVEC cells were co-transfected with WT FAS (FAS-3UTR-WT) or its mutant (FAS-3UTR-MUT), miRNA control (NC) or miR-135a-5p mimic (miR mimic) for 24 h; Firefly luciferase activity was normalized to Renilla luciferase activity; results are mean ± SD (n=3); **p<0.05 *vs* NC; ***p<0.01 *vs* NC.
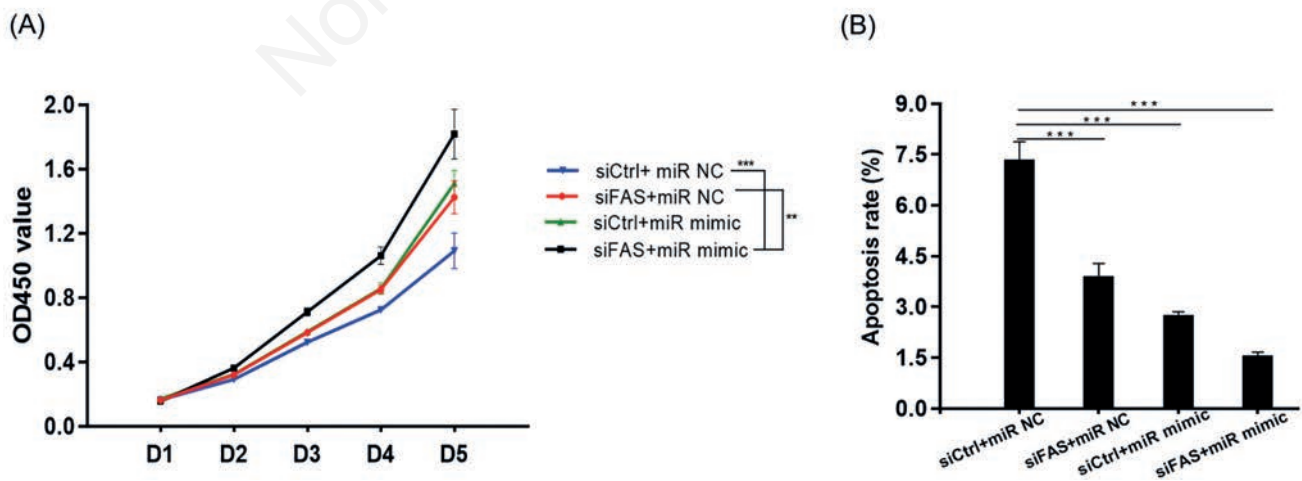
Figure 3. FAS knockdown and miR-130a-5p overexpression altered ox-LDL induced reduction of cell viability and apoptosis. A) The effect of siFAS and miR-130a-5p mimic on the ox-LDL-induced reduction of HUVEC viability was detected with CCK-8; **p<0.05 *vs* siFAS + miR NC; ***p<0.01 *vs* siCtrl + miR NC. B) The effect of siFAS and miR-130a-5p mimic on the ox-LDL-induced reduction of HUVEC apoptosis was determined by flow cytometry; results are mean ± SD (n=3); ***p<0.01 *vs* siCtrl + miR NC.

cantly decreased to a greater degree when compared with control group (Figure 4). Meanwhile, in ox-LDL treatment cells, the percentage of HUVECs in the S and G₂/M phases was remarkably increased than the control group (Figure 4). In addition, the percentage of S and G₂/M phases cells in siFAS and miR-130a-5p mimic group was more obviously enhanced than the control group (Figure 4).

Overall, these results suggested that the downregulation of FAS and upregulation of miR-130a-5p could lead to cell cycle arrest at the S and G$_2$/M phases.
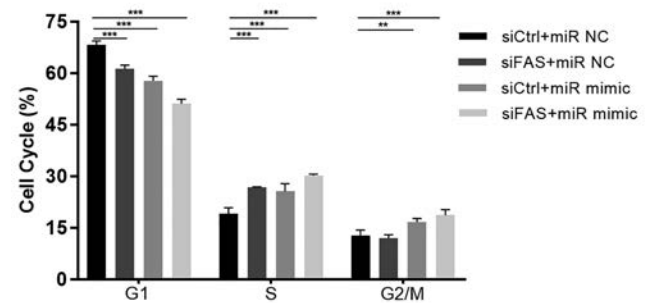
FAS knockdown and miR-130a-5p overexpression increased ox-LDL-induced cell proliferation reduction

We tested the alteration on the ox-LDL-induced reduction of cell proliferation after FAS knockdown or/and miR-130a-5p overexpression. Cell proliferation in live cells was slowly and significantly increased in D4 in ox-LDL treatment cells with siCtrl and miR NC (control group, Figure 5). Meanwhile, cell proliferation was significantly increased to a greater degree in both siFAS and miR NC (siFAS group), or siCtrl and miR-130a-5p mimic (miR-130-5p mimic group) in D4 compared with that of the control group. Whereas the cell proliferation of siFAS and miR-130a-5p mimic group was significantly increased to a greater degree when compared with the controls: the siFAS and miR-130a-5p mimic groups (Figure 5).
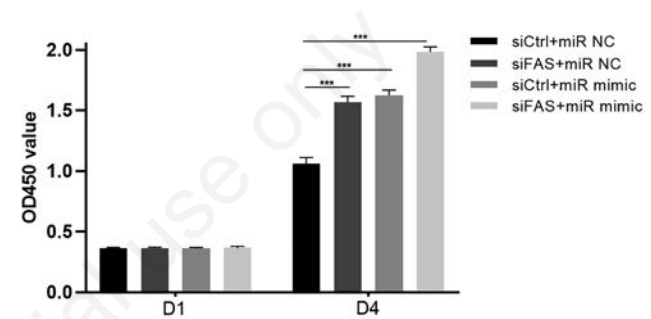
FAS knockdown and miR-130a-5p overexpression promoted ox-LDL-induced migration and invasion reduction

Enhanced migration and invasion are another key feature across the metastatic cascade. To assess the effect of FAS knockdown and miR-130a-5p overexpression on the migration and invasion of HUVEC cells, wound scratch and transwell assays were performed, respectively.
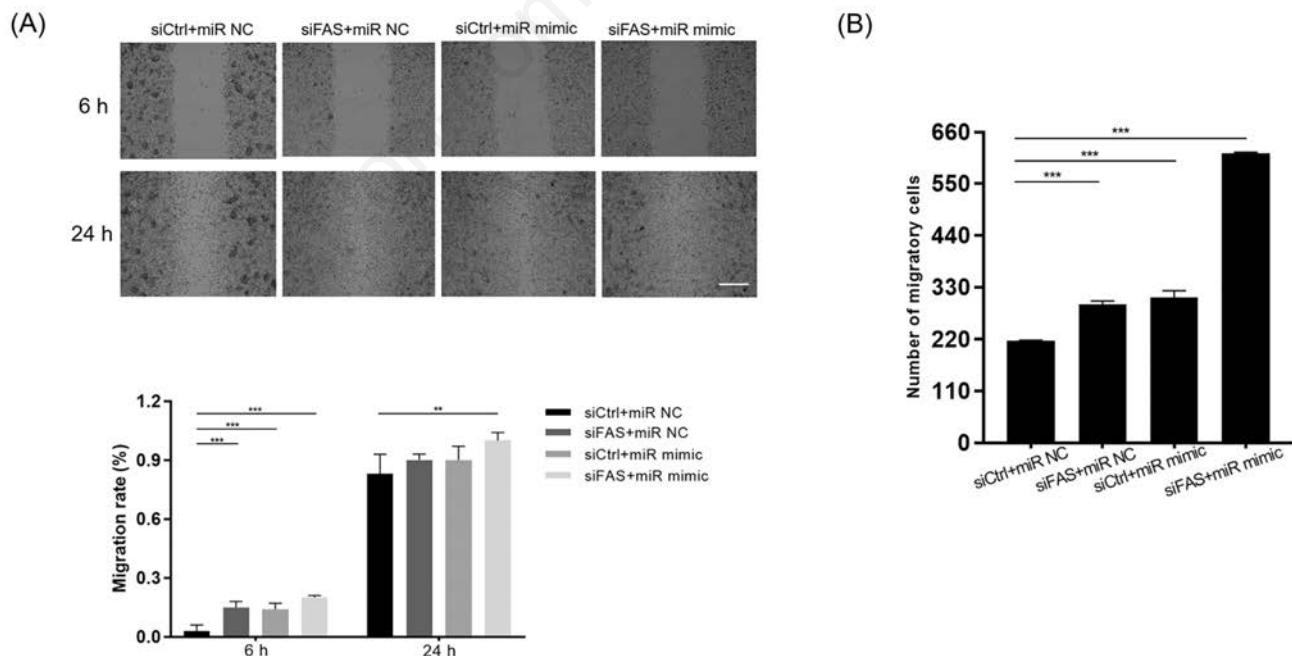
As shown in Figure 6 A,B, the rate of gap closure and invasion were significantly increased in the siFAS and miR-130a-5p mimic

Figure 4. FAS knockdown and miR-130a-5p overexpression effect on ox-LDL-induced cell cycle progression; results are mean ± SD (n=3); **p<0.05 *vs* siCtrl + miR NC; ***p<0.01 *vs* siCtrl + miR NC.

Figure 5. FAS knockdown and miR-130a-5p overexpression increased ox-LDL-induced reduction of cell proliferation, which was tested by using the EdU assay. Results are mean ± SD (n=3); ***p<0.01 *vs* siCtrl + miR NC.

Figure 6. FAS knockdown and miR-130a-5p overexpression promoted ox-LDL-induced reduction of migration and invasion. A) The rate of gap closure in scratch assay (scale bar: 200 μm) and invasion measured by transwell assay (B). Results are mean ± SD (n=3; **p<0.05 *vs* siCtrl + miR NC; ***p<0.01 *vs* siCtrl + miR NC.

groups compared with that of the control group, whereas the rate of gap closure and invasion of siFAS and miR-130a-5p mimic group was also significantly enhanced to a greater degree when compared with the siFAS and miR-130a-5p mimic control groups (Figure 6 A,B).

Discussion

In this study, our goal was to explore the potential important roles of miR-130a-5p and FAS during the progression of endothelial cell injury and provide the rationale for novel potential therapeutic tools of AS. We used ox-LDL to treat HUVEC cells and build up a cell modal of AS. Then we found that FAS was repressed by miR-130a-5p. In addition, FAS knockdown and miR-130a-5p overexpression was found to play important roles on ox-LDL induced reduction of cell viability, apoptosis, cell cycle progression, cell proliferation, migration and invasion.

miR-130a-5p has emerged as an important regulator in different human diseases. miR-130a-5p has been found to affect cell growth, migration and invasion by targeting CR1R *via* the Wnt/β-catenin signaling pathway in gastric carcinoma.[23] In addition, the miRNA-130a-5p/RUNX2/STK32A network modulates tumor invasive and metastatic potential in non-small cell lung cancer.[24] Moreover, FAM225A promotes sorafenib resistance in hepatocarcinoma cells by modulating the miR-130a-5p–CCNG1 interaction network.[25] In this study, we found that miR-130a-5p expression decreased as the dose of ox-LDL increased. FAS mRNA and miR-130a-5p expression levels are negatively correlated. In addition, miR-130a-5p overexpression was found to aggregate ox-LDL induced reduction of cell viability and apoptosis, cell cycle progression, cell proliferation, migration and invasion.

Currently, miRNAs and FAS have been reported to work together and play important roles in human diseases. MiR-196b-5p-mediated downregulation of FAS promotes NSCLC progression by activating IL6-STAT3 signaling.[26] MiR-19-3p has also been observed to induce tumor cell apoptosis via targeting FAS in rectal cancer cells.[27] Especially, miRNAs have been attracted more attention in AS study. miR-302c-3p has been reported to inhibit endothelial cell pyroptosis via directly targeting NOD-, LRR-and pyrin domain-containing protein 3 in AS.[28] miRNA-30e has been determined to regulate TGF-β-mediated NADPH oxidase 4-dependent oxidative stress by Snai1 in AS.[29] Although those previous studies, the biological activities of miR-130a-5p in AS still remains largely unknown. In this regard, we determined that miR-130a-5p contributed to the progression of endothelial cell injury by regulating of FAS. FAS is the direct target of miR-130a-5p. FAS knockdown and miR-130a-5p overexpression together were found to aggregate to a greater extent ox-LDL induced reduction of cell viability and apoptosis, cell cycle progression, cell proliferation, migration and invasion compared to FAS knockdown itself. However, further studies should be performed *in vivo*. Once the role of miR-103a-5p had been confirmed *in vivo*, miR-103a-5p would become a novel therapeutic target for AS patients.

References

1. Malakar AK, Choudhury D, Halder B, Paul P, Uddin A, Chakraborty S. A review on coronary artery disease, its risk factors, and therapeutics. J Cell Physiol 2019;234:16812-23.
2. Peng N, Meng N, Wang S, Zhao F, Zhao J, Su L, et al. An activator of mTOR inhibits oxLDL-induced autophagy and apoptosis in vascular endothelial cells and restricts atherosclerosis in apolipoprotein E(-)/(-) mice. Sci Rep 2014;4:5519.
3. Rahman MS, Woollard K. Atherosclerosis. Adv Exp Med Biol 2017;1003:121-44.
4. Suciu CF, Prete M, Ruscitti P, Favoino E, Giacomelli R, Perosa F. Oxidized low density lipoproteins: The bridge between atherosclerosis and autoimmunity. Possible implications in accelerated atherosclerosis and for immune intervention in autoimmune rheumatic disorders. Autoimmun Rev 2018;17:366-75.
5. Pedicino D, Giglio AF, Galiffa VA, Cialdella P, Trotta F, Graziani F, et al. Infections, immunity and atherosclerosis: pathogenic mechanisms and unsolved questions. Int J Cardiol 2013;166:572-83.
6. Trpkovic A, Resanovic I, Stanimirovic J, Radak D, Mousa SA, Cenic-Milosevic D, et al. Oxidized low-density lipoprotein as a biomarker of cardiovascular diseases. Crit Rev Clin Lab Sci 2015;52:70-85.
7. Wang R, Zhang Y, Xu L, Lin Y, Yang X, Bai L, et al. Protein inhibitor of activated STAT3 Suppresses oxidized LDL-induced cell responses during atherosclerosis in apolipoprotein E-deficient mice. Sci Rep. 2016;6:36790.
8. Ambros V. The functions of animal microRNAs. Nature 2004;431:350-5.
9. Si W, Shen J, Zheng H, Fan W. The role and mechanisms of action of microRNAs in cancer drug resistance. Clin Epigenetics 2019;11:25.
10. Sun D, Xiang G, Wang J, Li Y, Mei S, Ding H, et al. miRNA 146b-5p protects against atherosclerosis by inhibiting vascular smooth muscle cell proliferation and migration. Epigenomics 2020;12:2189-204.
11. Zhang F, Cheng N, Du J, Zhang H, Zhang C. MicroRNA-200b-3p promotes endothelial cell apoptosis by targeting HDAC4 in atherosclerosis. BMC Cardiovasc Disord 2021;21:172.
12. Liu F, Liu Y, Du Y, Li Y. MiRNA-130a promotes inflammation to accelerate atherosclerosis via the regulation of proliferator-activated receptor gamma (PPARgamma) expression. Anatol J Cardiol 2021;25:630-7.
13. Youssef EM, Elfiky AM, BanglySoliman, Abu-Shahba N, Elhefnawi MM. Expression profiling and analysis of some miRNAs in subcutaneous white adipose tissue during development of obesity. Genes Nutr 2020;15:8.
14. Mo JS, Alam KJ, Kang IH, Park WC, Seo GS, Choi SC, et al. MicroRNA 196B regulates FAS-mediated apoptosis in colorectal cancer cells. Oncotarget 2015;6:2843-55.
15. Fouque A, Debure L, Legembre P. The CD95/CD95L signaling pathway: a role in carcinogenesis. Biochim Biophys Acta 2014;1846:130-41.
16. Kischkel FC, Hellbardt S, Behrmann I, Germer M, Pawlita M, Krammer PH, et al. Cytotoxicity-dependent APO-1 (Fas/CD95)-associated proteins form a death-inducing signaling complex (DISC) with the receptor. EMBO J 1995;14:5579-88.
17. Luo L, Liang H, Liu L. Myristicin regulates proliferation and apoptosis in oxidized low-density lipoprotein-stimulated human vascular smooth muscle cells and human umbilical vein endothelial cells by regulating the PI3K/Akt/NF-kappaB sig-

nalling pathway. Pharm Biol 2022;60:56-64.

18. Yin Q, Fischer L, Noethling C, Schaefer WR. In vitro-assessment of putative antiprogestin activities of phytochemicals and synthetic UV absorbers in human endometrial Ishikawa cells. Gynecol Endocrinol 2015;31:578-81.

19. Arsic N, Bendris N, Peter M, Begon-Pescia C, Rebouissou C, Gadea G, et al. A novel function for Cyclin A2: control of cell invasion via RhoA signaling. J Cell Biol 2012;196:147-62.

20. Chen LM, Wang W, Lee JC, Chiu FH, Wu CT, Tai CJ, et al. Thrombomodulin mediates the progression of epithelial ovarian cancer cells. Tumour Biol 2013;34:3743-51.

21. Espada J, Matabuena M, Salazar N, Lucena S, Kourani O, Carrasco E, et al. Cryptomphalus aspersa mollusc eggs extract promotes migration and prevents cutaneous ageing in keratinocytes and dermal fibroblasts in vitro. Int J Cosmet Sci 2015;37:41-55.

22. Lee SJ, Kim WJ, Moon SK. Role of the p38 MAPK signaling pathway in mediating interleukin-28A-induced migration of UMUC-3 cells. Int J Mol Med 2012;30:945-52.

23. Xian X, Tang L, Wu C, Huang L. miR-23b-3p and miR-130a-5p affect cell growth, migration and invasion by targeting CB1R via the Wnt/beta-catenin signaling pathway in gastric carcinoma. Onco Targets Ther 2018;11:7503-12.

24. Ma F, Xie Y, Lei Y, Kuang Z, Liu X. The microRNA-130a-5p/RUNX2/STK32A network modulates tumor invasive and metastatic potential in non-small cell lung cancer. BMC Cancer. 2020;20:580.

25. Liu YT, Liu GQ, Huang JM. FAM225A promotes sorafenib resistance in hepatocarcinoma cells through modulating miR-130a-5p-CCNG1 interaction network. Biosci Rep 2020;40: BSR20202054.

26. Huang X, Xiao S, Zhu X, Yu Y, Cao M, Zhang X, et al. miR-196b-5p-mediated downregulation of FAS promotes NSCLC progression by activating IL6-STAT3 signaling. Cell Death Dis 2020;11:785.

27. Su YF, Zang YF, Wang YH, Ding YL. MiR-19-3p induces tumor cell apoptosis via targeting FAS in rectal cancer cells. Technol Cancer Res Treat 2020;19:1533033820917978.

28. Bai B, Yang Y, Ji S, Wang S, Peng X, Tian C, et al. MicroRNA-302c-3p inhibits endothelial cell pyroptosis via directly targeting NOD-, LRR- and pyrin domain-containing protein 3 in atherosclerosis. J Cell Mol Med 2021;25:4373-86.

29. Cheng Y, Zhou M, Zhou W. MicroRNA-30e regulates TGF-beta-mediated NADPH oxidase 4-dependent oxidative stress by Snai1 in atherosclerosis. Int J Mol Med 2019;43:1806-16.

OPEN ACCESS